Journal of Thermal Analysis and Calorimetry, Vol. 91 (2008) 3, 835–839

THERMAL CHARACTERIZATION OF METHYLTRIBUTYLAMMONIUM-SMECTITES

M. Önal and Y. Sarıkaya*

Ankara University, Faculty of Science, Department of Chemistry, Tando ğan, 06100 Ankara, Turkey

A sodium smectite (NaS) with a cation exchange capacity (CEC) of 1.08 mol kg^{-1} was intercalated with methyltributylammonium cation ($MTBA^+$) with proportions equivalent to 0.2, 0.4, 0.6, 0.8 and 1.0 times the CEC. The contents of adsorbed water and intercalated $MTBA^+$ in the prepared organosmectites (OSs) were determined by using the differential thermal analysis (DTA) and thermogravimetry (TG) curves. The adsorbed water of 8% in the NaS decreases greatly in OSs with the increase of the $MTBA^+$ content and reduces to 2.0% for the 1.0 CEC sample. This explains the gradual change of the NaS from hydrophilic to hydrophobic character. Thermal degradation of the intercalated $MTBA^+$ in OSs occurs approximately between 250–450°C. The oxidation of the formed charcoal to CO_2 occurs between 450–850°C. The intercalated $MTBA^+$ content for each OS is obtained from both the TG and carbon analysis. The results do not agree exactly, but both the results tend to increase by increasing initial content of the $MTBA^+$ in solution.

Keywords: *activation energy, degradation, hydrophilic-hydrophobic characterization, intercalation, organosmectites, thermal analysis*

Introduction

The major clay mineral in bentonites happen to be a form of smectite such as montmorillonite, saponite, nontronite, beidellite and hectorite [1, 2]. Smectite is a 2:1 layer clay mineral and has two silica tetrahedral (T) sheets bonded to a central alumina octahedral (O) sheet. The net negative charge of the 2:1 (TOT) layers arising from the isomorphic substitution in the octahedral sheets of Al^{3+} by Fe^{2+} and Mg^{2+} and in the tetrahedral sheets of Si^{4+} by Al^{3+} is balanced by the exchangeable cations such as Na^+ and Ca^{2+} located between the layers and around the edges [3–5]. The equivalent amount of exchangeable cations in one kilogram of smectite is defined as cation exchange capacity (CEC). Layer charge and CEC of smectites investigated have been determined by various techniques [6–14]. Smectites, as industrial minerals, have a wide range of uses [15–20].

Smectites known to be an efficient gellant for water systems are not effective in gelling in organic liquids [21–23]. It is known that a smectite having no swelling properties in organic liquids acquires a tendency to swell in various organic liquids after reaction with some tetraalkylammonium salts [24–26]. Such organophilic material obtained by the exchange of tetraalkylammonium cations (TAA^+) for inorganic interlayer cations may be called as organoclay, organobentonite, organosmectite, and organomontmorillonite [27–29]. The intercalated TAA^+ act as pillars which hold the 2:1 layers permanently apart [30–33]. Organosmectites (OS) are highly effective and used industrially in removing some organic pollutants from waste water [34–37].

The importance of organosmectites in science and industry is currently on increase. Recently, besides several application areas, organosmectites have been used in the synthesis of nanocomposites [38, 39]. When compared with other materials of the same purpose, organosmectite-based nanocomposites have a better strength, heat resistance and biodegradability besides decreased gas permeability and flammability [40–45]. The functional properties of these materials are strongly related to their microstructure and the thermal characteristics for many application areas [46, 47]. To investigate the thermal behavior of materials thermogravimetry (TG), differential thermal analysis (DTA), and differential scanning calorimetry (DSC) in combination with other techniques such as X-ray diffraction (XRD), Fourier transform infrared (FTIR) spectroscopy, Raman spectroscopy (RS), and nuclear magnetic resonance (NMR) are suitable [48–56]. In recent years thermal properties of organosmectites and their nanocomposites have been extensively investigated [57–71].

The aim of this study is to examine the thermal behavior of a $MTBA^+$-intercalated smectite by using only TG and DTA data. The content of intercalated $MTBA^+$ and the conversion of the hydrophilic smectite surface to an organophilic character were investigated on the bases of these data collected.

* Author for correspondence: onal@science.ankara.edu.tr

1388–6150/$20.00

Akadémiai Kiadó, Budapest, Hungary
Springer, Dordrecht, The Netherlands

Experimental

The sodium-rich smectite (NaS) was obtained from purification of Reşadiye (Tokat, Turkey) bentonite [72]. The original bentonite was separated into four fractions by successive decantation and precipitation from its aqueous suspensions. The final (NaS) suspension was used in the experiments. X-ray diffraction data showed that the NaS so obtained contains only a trace of opal-CT. The CEC is 1.08 eq kg^{-1}. The chemical formula is $Na_{0.265}K_{0.027}Ca_{0.025}$ $(Al_{1.528}Ti_{0.015}Fe^{3+}_{0.141}$ $Fe^{2+}_{0.093}$ $Mg_{0.188})$ $(Si_{3.939}Al_{0.061})O_{10}(OH)_2{\cdot}nH_2O$ [73]. This formula shows that the NaS concerned is virtually a sodium-rich montmorillonite. The surfactant used in this study, supplied from Merck Chemical Company, is methyltributylammonium chloride (MTBAC) with the chemical formula $[CH_3N(C_4H_9)_3]^+Cl^-$.

The methyltributylammonium smectite (MTBAS) were synthesized as follows: 10 g of the NaS dried at 105°C for 4 h was first dispersed in 500 mL of distilled water and then a 5% solution of MTBAC was added drop by drop until the pre-estimated quantity of MTBAC was reached. The obtained mixture was stirred at room temperature for 24 h. The amount of MTBAC added was varied from 0.2 to 1.0 CEC of the NaS. The molar content of the initial $MTBA^+$ is equal to those of the corresponding MTBAC and labeled as *x*. All MTBASs were washed until free of chloride anions against 0.1 M $AgNO_3$ solution dried at 60°C and ground to pass through a 0.074 mm (200 mesh) sieve. OS with 0.2 equivalent CEC was labeled OS2 and the others were named accordingly. These organosmectites were examined by XRD, FTIR spectroscopy and nitrogen adsorption–desorption techniques and the results were reported in a previous study [74]. The layer spacing for the air dried NaS is *d*(001)=1.21 nm and it increases from 1.26 to 1.58 nm by increasing $MTBA^+$ content from 0.2 to 1.0 CEC in the OSs.

The DTA and TG curves of the NaS and organosmectites were obtained using a Netzsch instrument Model 429 in air. The heating rate was 10 K min^{-1} and α-Al_2O_3 was used as inert material. The temperature was varied from 25 to 1000°C. The carbon content of the air dried samples were determined by an element-analyzer (LECO CHNS 932).

Results and discussion

DTA and TG curves of the samples

The DTA and TG curves of the NaS and prepared OSs are given in Figs 1 and 2, respectively, for the temperature range of 25–1000°C. For the NaS, the first and major endothermic change between 25 and 450°C with an overall mass loss of 8.0% is due to the dehydration of interparticle water, adsorbed water, and interlayer water (W). The second endothermic change between 450–850°C with the mass loss of 6.0% is originated from the dehydroxylation (DX) of the NaS. The exothermic change without mass loss over 850°C is assigned to amorphization of the NaS. The total mass losses (W+DX) and residue (RE) by heating up to 1000°C are 14.0% and 86.0%, respectively. Although the W% is changeable; the ratio DX/RE=6.0/86.0=0.0698 is expected to be constant for both, natural and treated smectites.

Thermal changes in the organosmectites may be approximately divided into five steps as indicated in Figs 1 and 2. These thermal steps are similar to those reported for tributylammonium smectite in a recent paper [75]. The first step between 25–250°C is attributed to the evolution of free water from the OSs. The mass loss (*W*) for each OS by this endothermic

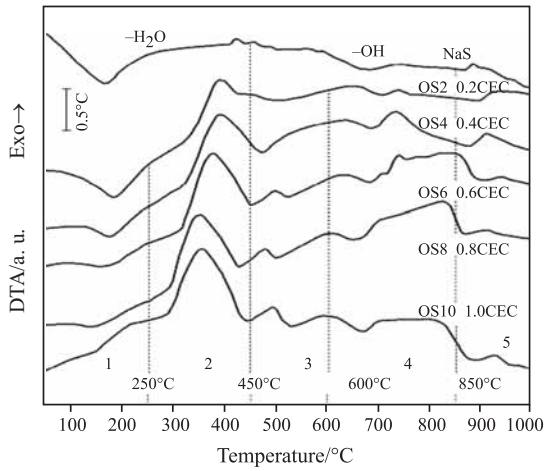

Fig. 1 The DTA curves of the NaS and organosmectites in the temperature range 25–1000°C

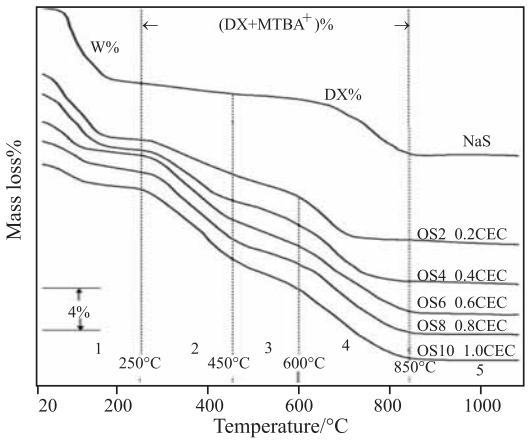

Fig. 2 The TG curves of NaS and organosmectites in the temperature range 25–1000°C, (W – adsorbed water, DX – dehydroxylation water, $MTBA^+$ – methyltributylammonium cation)

Table 1 Some physicochemical properties of the NaS and prepared organosmectites obtained from the thermogravimetry curves

Sample	*x*/CEC	W/%	DX+MTBA/%	DX/%	RE/%	$MTBA^+$/%	*y*/CEC
NaS	0	8.0	6.0	6.0	86.0	–	–
OS2	0.20	5.6	10.0	5.9	84.4	4.1	0.19
OS4	0.40	5.0	12.4	5.8	82.6	6.6	0.31
OS6	0.60	3.0	14.5	5.8	82.5	8.7	0.40
OS8	0.80	2.5	15.3	5.8	82.2	9.5	0.44
OS10	1.00	2.0	16.0	5.9	82.0	10.1	0.47

W – interparticle, adsorbed and interlayer water, DX – dehydroxylation water, $MTBA^+$ – methyltributylammonium cation, RE – residue at 1000°C, x – initial content of $MTBA^+$ as the times of CEC, y – intercalated content of $MTBA^+$ as the times of CEC in smectite

change is calculated from TG curve and given in Table 1. The second step between 250–450°C is assigned to the thermal degradation of the intercalated $MTBA^+$ by the exothermic oxidation reaction. Besides H_2O and CO_2, molecules charcoal is expected to form in this step. As seen in Fig. 2, the exothermic peak temperatures between 250–450°C slightly decrease while the basal spacing of the samples increase with the increasing of the $MTBA^+$ content. As the H_2O and CO_2 molecules tend to leave the larger-size interlayers more easily, these peaks are spread over a wide range of temperature as the $MTBA^+$ content and therefore the pore-size distribution-changes. The third step between 450–600°C mainly shows the oxidation of charcoal and formation of CO_2. The third step can not be exactly distinguished from the second and fourth steps. The formation of CO_2 must be accompanying the dehydroxylation (DX) of the NaS in the fourth step between 600–850°C. The fifth step above 850°C without any mass loss belongs only a thermal decrystallization of the remained NaS. The mass losses in the second, third and fourth steps can not be individually obtained from the TG curves. The total mass loss in these steps is due to the dehydroxylation (DX) of the NaS and degradation of the intercalated $MTBA^+$. The total mass losses ($DX+MTBA^+$) between 250–1000°C and also residues (RE) at 1000°C are calculated from the TG curves and given in Table 1.

The dehydroxylation mass loss (DX) for each OS was calculated from the constant ratio of DX/RE=0.0698 by using the known RE value and given in Table 1. The content of the intercalated $MTBA^+$ for each OS was obtained from the total of $DX+MTBA^+$ by using DX value calculated before and given in Table 1. The mass and mole number of $MTBA^+$ in 1 kg OS were calculated by the $(MTBA^+\%)\cdot 10$ and $(MTBA^+\%)\cdot 10/M^+$ relationships, respectively. The intercalated content of the $MTBA^+$ as times of the CEC for each OS was calculated from the relation

$$y=(MTBA^+\%)\cdot 10/(CEC)M^+ \quad (1)$$

where CEC of the NaS is 1.08 mol kg^{-1} and molar mass of the $MTBA^+$, $M^+=0.200$ kg mol^{-1}. The *y* values are given in Table 1. The relation between intercalated and initial contents (*y* and *x*) of the $MTBA^+$ is shown in Fig. 3. The degree of intercalation increases as the $MTBA^+$ content in the initial solution increases, but the rate of increase becomes less pronounced with higher values of *x*.

The carbon contents (C%) of the OSs are given in Table 2. The $MTBA^+$% in each OS are stoichiometrically calculated from C% and given in Table 2. The content of intercalated $MTBA^+$ was calculated from the Eq. (1). The relation between *y* and *x* is shown in Fig. 3.

As seen from Fig. 3, intercalated $MTBA^+$ contents found from C analysis is more than those obtained from TG data. This difference increases with the increasing content of intercalated $MTBA^+$. It was concluded that this difference arises from the experimental error imposed by TG-DTA, besides the uncertainty of the temperatures intervals of thermal steps.

Table 2 Intercalated $MTBA^+$ contents obtained from carbon analyzer (LECO CHNS 932)

Sample	C/%	$MTBA^+$/%	y/CEC
OS2	3.32	4.26	0.20
OS4	6.27	8.04	0.37
OS6	8.21	10.53	0.49
OS8	9.07	11.63	0.54
OS10	9.91	12.71	0.59

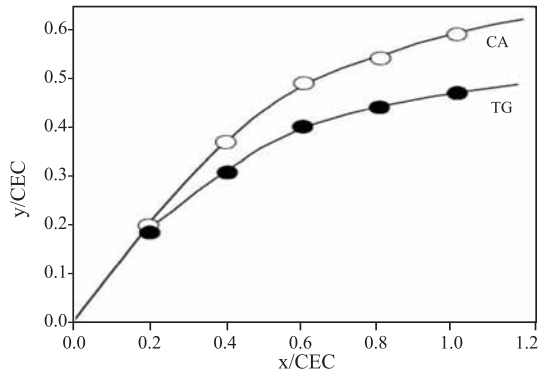

Fig. 3 The variation of the intercalated $MTBA^+$ content (y) with the used $MTBA^+$ content (x) in initial suspension

Hydrophilic–hydrophobic characters of the organosmectites

Water content of the organosmectites decreases with the intercalated $MTBA^+$ content as seen in Fig. 4. This shows that as we replace more of Na^+ by $MTBA^+$ the smectite surface transforms more, from hydrophilic to hydrophobic [76]. The W%–y plots drawn by using y values obtained from TG data and carbon analysis do not match exactly with each other. However, individual plots display the shape of a straight line. This $MTBA^+$ cations fixed on smectite surface form an organic partition nanophase. The hydrophobic (organophilic) nanophase functions like a bulk organic solvent which removes organic contaminants from waste waters.

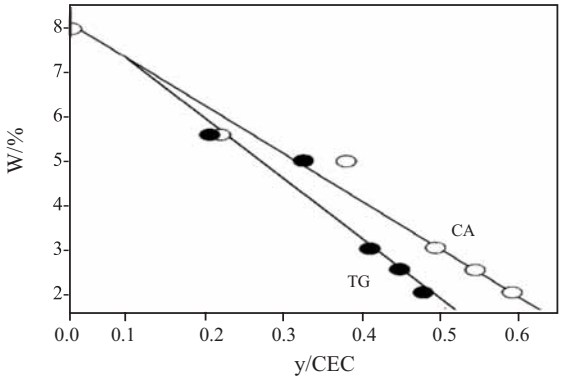

Fig. 4 The variation of the adsorbed water (W%) with the intercalated $MTBA^+$ content (y)

Conclusions

Thermal analysis gives significant information about the degradation of tetraalkylammonium cations intercalated between 2:1 layers of smectites. The ratio of the mass loss by dehydroxylation of smectite to the mass of residue at 1000°C remains approximately constant in natural and organosmectites. Based on this fact, the content of intercalated tetraalkylammonium cations can be calculated by using TG data besides carbon analysis. The intercalated organic cations degrade to give H_2O, CO_2 and charcoal as the temperature increases from 250 to 450°C. This charcoal is oxidized to give CO_2 up to 850°C.

Acknowledgements

The authors wish to thank to The Scientific and Technical Research Council of Turkey (TÜBITAK) for supporting this work under the project no: TBAG-2363 (103T138).

References

1 R. E. Grim, Clay Mineralogy, 2nd Ed., McGraw-Hill, New York 1968.
2 R. E. Grim and N. Güven, Bentonites, Geology, Mineralogy, Properties and Uses, Development in Sedimentology, Vol. 24, Elsevier, Amsterdam 1978.
3 H. H. Murray, Appl. Clay Sci., 5 (1991) 379.
4 H. H. Murray, Clay Miner., 34 (1999) 39.
5 H. H. Murray, Appl. Clay Sci., 17 (2000) 207.
6 G. Rytwo, C. Serben, S. Nir and L. Margulies, Clays Clay Miner., 39 (1991) 551.
7 G. Kahr and F. T. Madson, Appl. Clay Sci., 9 (1995) 327.
8 A. Czímerová, J. Bujdák and R. Dohrmann, Appl. Clay Sci., 34 (2006) 2.
9 S. Kaufhold, Appl. Clay Sci., 34 (2006) 14.
10 S. Petit, D. Righi and J. Madejová, Appl. Clay Sci., 34 (2006) 22.
11 R. Dohrmann, Appl. Clay Sci., 34 (2006) 31.
12 R. Dohrmann, Appl. Clay Sci., 34 (2006) 38.
13 R. Dohrmann, Appl. Clay Sci., 34 (2006) 47.
14 J. Bujdák, Appl. Clay Sci., 34 (2006) 58.
15 R. M. Barrer, Clays Clay Miner., 37 (1989) 385.
16 T. J. Pinnavia, Science, 220 (1983) 365.
17 E. Srasra, F. Bergaya, H. van Damme and N. K. Ariquib, Appl. Clay Sci., 4 (1989) 411.
18 E. Gamiz, J. Linares and R. Delgado, Appl. Clay Sci., 6 (1992) 359.
19 R. S. Varma, Tetrahedron, 58 (2002) 1235.
20 F. Bergaya, B. K. G. Theng and G. Lagaly, Eds, Handbook of Clay Science. Elsevier, 2006.
21 K. Norrish, Faraday Discuss., 18 (1954) 120.
22 P. F. Low, Soil Sci. Soc. Am. J., 43 (1979) 651.
23 P. F. Luckham and S. Rossi, Adv. Colloid Interface, 82 (1999) 43.
24 J. W. Jordan, J. Phys. Chem., 53 (1949) 294.
25 J. W. Jordan, B. J. Hook and C. M. Finlayson, J. Phys. Chem., 54 (1950) 1196.
26 L. P. Meier, R. Nueesch and F. T. Madsen, J. Colloid Interface Sci., 238 (2001) 24.
27 M. M. Mortland, Adv. Agron., 22 (1970) 75.
28 B. K. G. Theng, The Chemistry of Clay-Organic Reactions. Adam Hilgar, London 1974.
29 M. Önal and Y. Sarıkaya, Colloid Surfaces A., 296 (2007) 216.

30 W. W. Emerson, Nature, 180 (1957) 48.
31 J. L. Bonczek, W. G. Harris and P. Nkedi-Kizza, Clays Clay Miner., 50 (2002) 11.
32 S. Y. Lee and S. J. Kim, Clays Clay Miner., 50 (2002) 435.
33 V. Luptáková and G. Plesh, Clay Miner., 40 (2005) 295.
34 S. A. Boyd, J. F. Lee and M. M. Mortland, Nature, 333 (1988) 345.
35 S. A. Boyd, M. M. Mortland and C. T. Chiou, Soil Sci. Soc. Am. J., 52 (1988) 652.
36 Y. Chun, G. Sheng and S. A. Boyd, Clays Clay Miner., 51 (2003) 415.
37 M. O. Adebajo, R. L. Frost, J. T. Kloprogge and O. Carmody, J. Porous Mater., 10 (2003) 159.
38 P. C. LeBaron, Z. Wang and T. J. Pinnavaia, Appl. Clay Sci., 15 (1999) 11.
39 S. S. Ray and M. Okamoto, Prog. Polym. Sci., 28 (2003) 1539.
40 Y. Kojima, A. Usuki, M. Kavasumi, Y. Fukushima, A. Okada, T. Kurauchi and O. Kamigaito, J. Mater. Res., 8 (1993) 1179.
41 J. W. Gilman, T. Kashiwagi and J. D. Lichtenhan, Sampf J., 33 (1997) 40.
42 J. W. Gilman, Appl. Clay Sci., 15 (1999) 31.
43 R. A. Vaia, G. Price, P. N. Ruth, H. T. Nojuyen and J. Lichtenhan, Appl. Clay. Sci., 15 (1999) 67.
44 J. W. Gilman, C. L. Jackson, A. B. Morgan, R. Harris, Jr., E. Manias, E.P. Giannelis, M. Wuthenow, D. Hilton and S. H. Phillips, Chem. Mater., 12 (2000) 1866.
45 S. R. Sinha, K. Yamada, M. Okamoto and K. Ueda, Nanotech. Lett., 2 (2002) 1093.
46 C. I. Park, M. H. Kim and O. O. Park, Polymer, 45 (2004) 1267.
47 H. Krump, A. S. Luyt and I. Hudee, Mater. Lett., 60 (2006) 2877.
48 E. Kristóf-Makó and A. Z. Juhász, Thermochim. Acta, 342 (1999) 105.
49 Y. Sarıkaya, M. Önal, B. Baran and T. Alemdaroğlu, Clays Clay Miner., 48 (2000) 557.
50 R. L. Frost and M. L. Weier, Thermochim. Acta, 406 (2003) 221.
51 R. L. Frost, M. L. Weier, M. E. Clissold, P. A. Williams and J. T. Kloprogge, Thermochim. Acta, 407 (2003) 1.
52 R. L. Frost, E. Horváth, E. Makó, J. Kristóf and A. Rédey, Thermochim. Acta, 408 (2003) 103.
53 H. Noyan, M. Önal and Y. Sarıkaya, Clays Clay Miner., 54 (2006) 375.
54 N. Yener, M. Önal, G. Üstünışık and Y. Sarıkaya, J. Therm. Anal. Cal., 88 (2007) 813.
55 H. Bayram, M. Önal, G. Üstünışık and Y. Sarıkaya, J. Therm. Anal. Cal., 89 (2007) 169.
56 M. Önal and Y. Sarıikaya, J. Therm. Anal., Cal. OnlineFirst, DOI: 10.1007/s10973-005-7799-9.
57 W. Xie, Z. M. Gao, K. L. Liu, W. P. Pan, R. Vaia, D. Hunter and A. Singh, Thermochim. Acta, 339 (2001) 367.
58 W. Xie, Z. M. Gao, W. P. Pan, D. Hunter, A. Singh and R. Vaia, Chem. Mater., 13 (2001) 2979.
59 W. Xie, R. C. Xie, W. P. Pan, D. Hunter, B. Koene, L. S. Tan and R. Vaia, Chem. Mater., 14 (2002) 4837.
60 Y. Q. Li and H. Ishida, Chem. Mater., 14 (2002) 1398.
61 V. Balek, Z. Malek, U. Ehrlicher, K. Györyová, G. Matuschek and S. Yariv, Appl. Clay Sci., 21 (2002) 295.
62 K. P. Pramoda, T. Liu, Z. Liu, C. He and H. J. Sue, Polym. Degrad. Stab., 81 (2003) 47.
63 Y. Xi, Z. Ding, H. He and R.L. Frost, J. Colloid Interface Sci., 277 (2004) 116.
64 S. Yariv, Appl. Clay Sci., 24 (2004) 225.
65 S. Yariv and L. Lapides, J. Therm. Anal. Cal., 80 (2005) 11.
66 Y. Xi, W. Martens, H. He and R. L. Frost, J. Therm. Anal. Cal., 81 (2005) 91.
67 F. Kooli and P. C. M. M. Magusin, Clay Miner., 40 (2005) 233.
68 H. He, Z. Ding, J. Zhu, P. Yuan, Y. Xi, D. Yang and R. L. Frost, Clays Clay Miner., 53 (2005) 287.
69 J. C. A. A. Roelofs and P.H. Berben, Appl. Clay Sci., 33 (2006) 13.
70 M. Önal and Y. Sarıkaya, J. Therm. Anal. Cal., OnlineFirst, DOI: 10.1007/s10973-007-8319-x.
71 M. Önal, Y. Sarıkaya, T. Alemdaroğlu and İ. Bozdoğan, Turk. J. Chem., 27 (2003) 683.
72 M. Önal, Commun. Fac. Sci. Uni. Ank., 52 (2006) 1.
73 C. B. Hedley, G. Yuan and B. K. G. Theng, Appl. Clay Sci., 35 (2007) 180.
74 M. Önal and Y. Sarıkaya, Colloids Sur., in press.
75 D. Ovadyahu, I. Lapides and S. Yariv, J. Therm. Anal. Cal., 87 (2007) 125.
76 W. H. Slabaugh and L.S . Carter, J. Colloid Interface Sci., 27 (1968) 235.

Received: March 21, 2007
Accepted: July 18, 2007

DOI: 10.1007/s10973-007-8456-2